J. Fluid Mech. (1980), *vol.* 101, *part* 4, *pp.* 737–758
Printed in Great Britain

Thermophoresis of particles in a heated boundary layer

By L. TALBOT

Mechanical Engineering Department and Lawrence Berkeley Laboratory, University of California

R. K. CHENG, R. W. SCHEFER

Lawrence Berkeley Laboratory

AND D. R. WILLIS

Mechanical Engineering Department, University of California

(Received 15 October 1979)

A laser-Doppler velocimeter (LDV) study of velocity profiles in the laminar boundary layer adjacent to a heated flat plate revealed that the seed particles used for the LDV measurements were driven away from the plate surface by thermophoretic forces, causing a particle-free region within the boundary layer of approximately one half the boundary-layer thickness. Measurements of the thickness of this region were compared with particle trajectories calculated according to several theories for the thermophoretic force. It was found that the theory of Brock, with an improved value for the thermal slip coefficient, gave the best agreement with experiment for low Knudsen numbers, $\lambda/R = O(10^{-1})$, where λ is the mean free path and R the particle radius.

Data obtained by other experimenters over a wider range of Knudsen numbers are compared, and a fitting formula for the thermophoretic force useful over the entire range $0 \leqslant \lambda/R \leqslant \infty$ is proposed which agrees within 20 % or less with the majority of the available data.

1. Introduction

The application of laser-Doppler velocimetry (LDV) to gas flows requires the introduction of seeding particles as light scatterers. For accurate LDV measurements, the seed particles must follow the fluid flow faithfully. Workers in the field, as for example, Durst, Melling & Whitelaw (1976) have called attention to many of the kinds of forces acting on seed particles which might cause their motions to depart from the fluid motion. The force of chief concern in most applications is the viscous drag force (which, of course, causes the particles to follow the fluid motion), but others, such as electrostatic, gravity, centrifugal, acoustic, diffusiophoretic and thermophoretic forces could conceivably play a role in influencing particle motion. In what follows, we describe an experiment in which the thermophoretic force plays a dominant role, and in fact severely limits the application of the LDV technique. However, the experiment does provide an opportunity to estimate the magnitude of the thermophoretic force and to compare it with theoretical predictions under conditions which apparently have not been investigated before. The literature on thermophoresis, which is rather

0022-1120/80/4562-2240 $02.00

extensive, contains a number of conflicting results, both theoretical and experimental. We have therefore, in addition to reporting our own results, undertaken what we hope will be a useful review of the existing theoretical and experimental work on this problem.

2. Theoretical background

Thermophoresis is the term describing the phenomenon wherein small particles, such as soot particles, aerosols or the like, when suspended in a gas in which there exists a temperature gradient ∇T, experience a force in the direction opposite to that of ∇T. A common example of the phenomenon is the blackening of the glass globe of a kerosene lantern; the temperature gradient established between the flame and the globe drives the carbon particles produced in the combustion process towards the globe, where they deposit. Thermophoresis is of practical importance in many industrial applications, such as in thermal precipitators, which are sometimes more effective than electrostatic precipitators in removing sub-micron-sized particles from gas streams.

The fundamental physical processes responsible for the phenomenon of thermophoresis were first investigated by Maxwell (cf. Kennard 1938), in an attempt to explain the radiometer effect. Maxwell showed that, at an unequally heated solid boundary in contact with a gas, if the mean free path is not negligibly small in comparison to a characteristic dimension of the solid, molecules impinging obliquely on a small element of area of the boundary will deliver more tangential (and also normal) momentum to the wall if they come from the hotter region of the gas than if they come from the colder region (unless the reflexion is specular). The net result of the unequal tangential momentum transfer is that a shear stress is exerted by the gas on the wall in the direction opposite to $\partial T/\partial s$, the temperature gradient parallel to the wall in the gas. Also, since an equal and opposite shear stress is exerted by the wall upon the gas, a flow of the gas adjacent to the wall, called thermal slip or thermal creep, occurs in the direction toward the hotter region, unless a pressure gradient is imposed to resist the motion.

One of the earliest attempts to apply these ideas to the calculation of forces on spherical particles in a gas at rest in which there exists a temperature gradient is that of Epstein (1929) who derived expressions for the thermophoretic force and the velocity acquired by the particle in the slip flow regime (Knudsen number $\lambda/R \lesssim 1$).† For this regime Epstein derived the following expression for the thermophoretic force $\mathbf{F}_T$ on a spherical particle,

$$\mathbf{F}_T = -\frac{9\pi\mu\nu R\nabla T}{T_0}\left(\frac{k_g}{k_p+2k_g}\right) = -9R^2\nabla T\left(\frac{2\pi\mathscr{R}}{T_0}\right)^{\frac{1}{2}}\mu\frac{\lambda}{R}\left(\frac{k_g/k_p}{1+2k_g/k_p}\right) \tag{1}$$

in which R is the radius of the particle, μ is the gas viscosity, ρ the gas density, $\nu = \mu/\rho$, T_0 the mean gas temperature in the vicinity of the particle, ∇T the temperature gradient in the gas, and k_g and k_p the thermal conductivities of the gas and particle respectively.‡

† We shall use for the mean free path the viscosity-based value, $\lambda = 2\mu/\rho\bar{c}$ with $\bar{c} = (8\mathscr{R}T/\pi)^{\frac{1}{2}}$ the mean molecular speed, and $\mathscr{R}$ the specific gas constant.

‡ In the case of polyatomic gases, one should use the 'translational' thermal conductivity, which in the simple kinetic theory is given by $k_g = \frac{15}{4}\mu\mathscr{R}$.

We shall see shortly how this result is related to that obtained from a more complete theory.

Epstein's result has been found to be in reasonably good agreement with experiments for $\lambda/R \lesssim 1$ for particles of low thermal conductivity, such that $k_g/k_p \sim O(1)$, but it seriously underestimates the thermal force on particles of high thermal conductivity, $k_p \gg k_g$, which according to (1) should experience much smaller forces (cf. Schadt & Cadle 1961). For example, thermophoretic forces on sodium chloride particles nearly two orders of magnitude larger than predicted by (1) have been reported by Schadt & Cadle and Derjaguin, Storozhilova & Rabinovich (1966).

A number of attempts have been made to improve upon the Epstein analysis in order to resolve the discrepancy between theory and experiment for high thermal conductivity particles. These attempts fall into four categories:

(i) 'hydrodynamic' analysis based on Navier–Stokes–Fourier theory, with slip-corrected boundary conditions;

(ii) analysis based on higher-order kinetic theory approximations to the continuum equations and boundary conditions;

(iii) analysis which employs phenomenological equations based on postulates of irreversible thermodynamics;

(iv) analysis based on the solution of the Boltzmann or BGK equations.

Of these approaches, the first is the simplest (and, as we shall see, the one which yields the most satisfactory results); hence it will be of use to outline briefly the method employed.

The hydrodynamic analysis was first carried out in a complete form by Brock (1962). Here we give a simplified version of his analysis. The problem is posed as follows. An ambient temperature distribution in the gas is assumed of the form (taking the temperature gradient in the gas to be in the x direction):

$$(T_g)_{r \gg R} = T_0 + (\nabla T)_x r \cos\theta, \tag{2}$$

where spherical polar co-ordinates r, θ with the origin at the centre of the stationary spherical particle are employed, and θ is measured from the positive x axis. The temperature fields in the gas (neglecting gas convection effects as small) and in the particle are both assumed to obey Laplace's equation,

$$\nabla^2 T_g = \nabla^2 T_p = 0, \tag{3}$$

together with the heat flux boundary condition at the surface of the sphere

$$k_g \left(\frac{\partial T_g}{\partial r}\right)_{r=R} = k_p \left(\frac{\partial T_p}{\partial r}\right)_{r=R} \tag{4}$$

and the temperature-jump boundary condition

$$(T_g - T_p)_{r=R} = C_t \lambda \left(\frac{\partial T_g}{\partial r}\right)_{r=R}, \tag{5}$$

where C_t is a numerical factor of order unity which must be obtained from kinetic theory. Its actual value as well as those of other boundary condition coefficients will be given subsequently.

The gas velocity field in the neighbourhood of the sphere is assumed to be governed

by the Navier–Stokes equations in the Stokes approximation. Using the Stokes stream function ψ we have

$$\left(\frac{\partial^2}{\partial r^2}+\frac{1}{r^2}\frac{\partial^2}{\partial\theta^2}-\frac{\cot\theta}{r^2}\frac{\partial}{\partial\theta}\right)^2\psi=0, \tag{6}$$

$$u_r=-\frac{1}{r^2\sin\theta}\frac{\partial\psi}{\partial\theta}, \quad u_\theta=\frac{1}{r\sin\theta}\frac{\partial\psi}{\partial r}, \tag{7}$$

with the boundary condition at $r\to\infty$ being

$$u_r=U\cos\theta, \quad u_\theta=-U\sin\theta, \tag{8}$$

where U is the free-stream velocity, assumed to be in the x direction. The radial velocity boundary condition at the surface of the sphere is the usual one,

$$(u_r)_{r=R}=0. \tag{9a}$$

However, the tangential velocity boundary condition, incorporating the effects of velocity slip and thermal slip, is

$$(u_\theta)_{r=R}=C_m\lambda\left[r\frac{\partial}{\partial r}\left(\frac{u_\theta}{r}\right)+\frac{1}{r}\frac{\partial u_r}{\partial\theta}\right]_{r=R}+\frac{C_s\nu}{RT_0}\left(\frac{\partial T_g}{\partial\theta}\right)_{r=R}. \tag{9b}$$

The first term on the right-hand side is the velocity slip correction boundary condition, with C_m being the momentum exchange coefficient. The second term represents the contribution of thermal slip to the gas velocity at the surface of the sphere, C_s being the thermal slip coefficient. It is this term which couples the temperature distributions in the gas and particle with the velocity field. Both C_m and C_s are numerical factors of order unity which must be obtained from kinetic theory.

The system of equations and boundary conditions (2)–(9), when solved for the force F in the x direction on the sphere, yields the result

$$F=F_V+F_T=6\pi\mu RU\left(\frac{1+2C_m\dfrac{\lambda}{R}}{1+3C_m\dfrac{\lambda}{R}}\right)-\frac{12\pi\mu\nu RC_s\left(\dfrac{k_g}{k_p}+C_t\dfrac{\lambda}{R}\right)\dfrac{(\nabla T)_x}{T_0}}{\left(1+3C_m\dfrac{\lambda}{R}\right)\left(1+2\dfrac{k_g}{k_p}+2C_t\dfrac{\lambda}{R}\right)}. \tag{10}$$

The first term on the right-hand side of (10) is F_V, the familiar Basset (1888) slip correction to the Stokes viscous drag formula. The Basset formula is accurate only for $\lambda/R\lesssim 0{\cdot}1$, and experiments for $\lambda/R<1$ favour the Stokes–Cunningham expression

$$F_V=\frac{6\pi\mu UR}{1+A\lambda/R}, \tag{11a}$$

which in actuality is a low-Knudsen-number approximation to the Millikan drag formula

$$F_V=\frac{6\pi\mu UR}{1+\dfrac{\lambda}{R}(A+Be^{-CR/\lambda})} \tag{11b}$$

in which the constants have the values $A=1{\cdot}20$, $B=0{\cdot}41$, $C=0{\cdot}88$, when the mean free path is defined as $\lambda=2\mu/\rho\bar{c}$.

The second term on the right-hand side of (10) is F_T, the thermophoretic force on

the spherical particle caused by the thermal slip effect. We note that F_T is in the negative-x direction, opposite to the direction of ∇T. If F_V and F_T are the only forces acting on the particle, then $F_V + F_T = 0$, and the value of U which yields this equality, the thermophoretic velocity U_T, is thus (with a minus sign added to change the frame of reference to that of the particle moving with respect to a stationary gas)

$$U_T = -\frac{2C_s\nu\left(\frac{k_g}{k_p}+C_t\frac{\lambda}{R}\right)\frac{(\nabla T)_x}{T_0}}{\left(1+2C_m\frac{\lambda}{R}\right)\left(1+2\frac{k_g}{k_p}+2C_t\frac{\lambda}{R}\right)}. \tag{12}$$

Although U_T is the quantity of concern to many investigators dealing with thermophoresis, in the general case when the particle may be undergoing acceleration or deceleration, or subjected to additional forces, $F_T + F_V \neq 0$ and both force components must be separately identified.

The expression for F_T contained in (10) was first obtained by Brock. Although he chose reasonable values for C_m and C_t (the best kinetic theory values for complete accommodation appear to be $C_m = 1{\cdot}14$, $C_t = 2{\cdot}18$, obtained by Loyalka & Ferziger 1967, Loyalka 1968), he used the value $C_s = \frac{3}{4}$, a value first obtained by Maxwell on the assumption that the distribution function in the bulk of the gas held all the way to the wall. More refined kinetic theory analysis by Ivchenko & Yalamov (1971) yielded the result $C_s = 1{\cdot}17$, for complete thermal accommodation, a value in substantial agreement with other kinetic-theory analyses.

Brock's result, with $C_s = \frac{3}{4}$, is found not to be in good agreement with experiment for particles of high thermal conductivity, although the discrepancy is much less than that obtained using the Epstein result. The latter, incidentally, may be seen to be a limiting form of Brock's result. If we take $k_g/k_p \gg \lambda/R$, which could be the case for particles of low thermal conductivity in the near-continuum regime, then with $C_s = \frac{3}{4}$ we obtain from the second term on the right-hand side of (10) the Epstein result (1). This explains why Epstein's result was generally accepted for many years, until data on particles for which $k_g/k_p \ll 1$ became available. Epstein's formula is in fact the formal limit $\lambda/R \to 0$ of the hydrodynamic theory. However, for particles of high thermal conductivity, $k_g/k_p \ll 1$, we observe that as soon as λ/R departs significantly from zero the λ/R term in the numerator of F_T will dominate over the term k_g/k_p, and F_T will be widely different from the Epstein limit. As an example, for sodium chloride particles in air, $k_g/k_p \approx 0{\cdot}004$, and hence even for λ/R as small as 10^{-2} the term in λ/R is the controlling one.

The Brock analysis, being based on the continuum equations with slip-corrected boundary conditions, can be expected to be applicable, roughly speaking, only for $\lambda/R \lesssim 0{\cdot}1$, since this is the limit of applicability of the Basset drag formula. In an attempt to extend the theory to higher Knudsen numbers Dwyer (1967) calculated F_T according to the 13-moment equations of Grad. He found fair agreement with experiment for particles of low thermal conductivity, but found that the analysis predicted an initial reversal of the force F_T in the near-continuum regime for particles of high thermal conductivity, because of a property of the 13-moment equations wherein heat transfer normal to a boundary gives rise to normal stresses on the boundary. This reversal in F_T, which is also predicted by Sone & Aoki (1977), is not observed in the experiments.

Vestner, Kübel & Waldmann (1975) used a set of moment equations similar to those employed by Dwyer, but with different boundary conditions which involved unknown surface interaction coefficients, and which they determined by fitting to experimental data. Thus a self-consistent test of their results is not possible.

A quite different approach was used by Derjaguin & Yalamov (1965, 1966) who presented a theory of thermophoresis based on an application of irreversible thermodynamics and Onsager's reciprocity relations, first to the problem of thermo-molecular pressure drop in a capillary, and then extended by (questionable) analogy to a porous partition of spheres. They obtain for the thermophoretic velocity

$$U_T = \frac{-3\nu}{T_0}(\nabla T)_x \frac{\left(\frac{k_g}{k_p} + C_t\frac{\lambda}{R}\right)}{\left(1 + 2\frac{k_g}{k_p} + 2C_t\frac{\lambda}{R}\right)}. \tag{13}$$

It is seen that this expression is similar to (12), except for missing the factor

$$(1 + 2C_m\lambda/R),$$

if $C_s = 1{\cdot}5$. The corresponding thermophoretic force would be obtained by inserting this expression for the velocity U_T into the Basset drag formula.

Derjaguin & Yalamov are critical of Brock's work but for totally unjustifiable reasons, since it is a self-consistent first-order slip calculation whose only flaw is the use of Maxwell's first estimate for the value of C_s. Indeed, it is probably unfair to call this a flaw, since, at the time of Brock's analysis, a better theoretical value for C_s was not available. They also make a statement regarding 'the falseness of the very foundations of Epstein's theory...', which as was shown earlier is in fact a particular limit of the hydrodynamic theory. It is of course quite a different matter to question whether a first-order theory adequately describes a particular phenomenon, than to assert that such a theory is fundamentally incorrect. It may be noted that, on theoretical grounds, the information derived from analysis based on the Onsager relations cannot exceed that obtained at the Navier–Stokes level of approximation within the framework of kinetic theory, since the assumed linear relationships between fluxes and gradients are valid only to this approximation. Moreover, irreversible thermodynamics yields no information on the surface interaction coefficients.

In the fourth category of analysis, that of the solution of the Boltzmann equation itself, we call attention to the analysis by Gorelov (1976) who solved numerically the linearized Boltzmann equation for the problem of the thermophoretic force on a sphere over the range $0{\cdot}1 \lesssim \lambda/R \leqslant \infty$, for two cases, $k_g/k_p = 0{\cdot}2$ and $k_g/k_p = 0{\cdot}002$, values typical of low-conductivity and high-conductivity particles, respectively. For the former case, the 'reduced thermophoretic force', $F_T/F_{T\infty}$ (where $F_{T\infty}$ is the free-molecular Waldmann value) varied monotonically from its minimum value, at the lowest value of λ/R calculated, to unity. For the high-conductivity case, however, there is the suggestion that in the vicinity of $\lambda/R = 0{\cdot}1$, F_T may be very slightly positive. We shall discuss subsequently the comparison between Gorelov's results and experiment.

3. A fitting formula

It would of course be desirable to have a simple expression for the thermophoretic force (or velocity) which could be employed over the entire range of Knudsen number $0 \leqslant \lambda/R \leqslant \infty$. However, it seems unlikely that this will be achievable through theoretical analysis. A much simpler approach, one which has been successful in other rarefied gasdynamics problems, is that of constructing an interpolation formula which matches the theory in the near-continuum and free molecular (collisionless) limits.

Springer (1970) employed this method to obtain a rather complicated formula which agreed reasonably well with experiment. However, he used for the slip flow limit a data-fitting equation proposed by Jacobson & Brock (1965) which, because it employed the Maxwell value for C_s, requires for best fit an unrealistic value for C_t, and also the specification of an undefined numerical constant. In what follows, a simpler result is presented.

The collisionless limit for F_T (Waldmann 1959, 1961) is, for complete thermal accommodation (see appendix),

$$\lim_{\lambda/R\to\infty} F_T \equiv F_{T\infty} = -\frac{32}{15}\frac{R^2}{\bar{c}}k_g(\nabla T)_x = -2\pi\mu\nu\frac{R^2}{\lambda}\frac{(\nabla T)_x}{T_0} \tag{14}$$

and the near-continuum limit is, from Brock,

$$F_T = -\frac{12\pi\mu\nu RC_s\left(\frac{k_g}{k_p}+C_t\frac{\lambda}{R}\right)\frac{(\nabla T)_x}{T_0}}{\left(1+3C_m\frac{\lambda}{R}\right)\left(1+2\frac{k_g}{k_p}+2C_t\frac{\lambda}{R}\right)}. \tag{15}$$

Now, although there is no mathematical justification for doing so, if we examine the limit of (15) as $\lambda/R \to \infty$, we find fortuitously that, except for the multiplicative factor (C_s/C_m), it is identical to (14). Since $C_s/C_m = 1{\cdot}17/1{\cdot}14 = 1{\cdot}03$, only a 3 % error is involved in using (15) in the limit $\lambda/R \to \infty$, and this suggests that (15) itself might represent a useful interpolation formula. In fact, a value of $C_s = 1{\cdot}14$, which would yield exact agreement with the Waldmann formula in the limit $\lambda/R \to \infty$, is well within the range of experimental and theoretical results. (Loyalka & Cipolla 1971 obtain the value $C_s = 1{\cdot}149$ from analysis based on the BGK model. Also, see Annis 1972 for a comprehensive summary of theoretical and experimental values of C_s.)

To obtain an expression for the thermophoretic velocity which might be useful over the entire range of Knudsen number, then, we can equate F_T to the Millikan drag formula, (11*b*), and changing the sign of U as before we obtain, for the thermophoretic velocity,

$$U_T = -\frac{2C_s\nu\left(\frac{k_g}{k_p}+C_t\frac{\lambda}{R}\right)\left[1+\frac{\lambda}{R}(A+Be^{-CR/\lambda})\right]\frac{(\nabla T)_x}{T_0}}{\left(1+3C_m\frac{\lambda}{R}\right)\left(1+2\frac{k_g}{k_p}+2C_t\frac{\lambda}{R}\right)}. \tag{16}$$

The fitting formula (15) has been compared with the results calculated by Gorelov. For the 'low-conductivity' case, $F_T/F_{T\infty}$ as given by (15) agrees (within the accuracy to which his graph can be read) almost exactly with Gorelov's result for $k_g/k_p = 0{\cdot}2$. It does not agree very well with Gorelov's results for $k_g/k_p = 0{\cdot}002$. However, as will be seen, (15) is apparently in better agreement with experiment for $k_g/k_p \ll 1$ than Gorelov's results.

4. Experimental background

Most recent experimental determinations of the thermophoretic force or velocity have been carried out by one of two methods. One method employs a modified Millikan cell (Rosenblatt & LaMer 1946; Schmitt 1959; Schadt & Cadle 1961) wherein a charged particle is held at rest or its velocity measured under the combined action of gravity, thermal and electrostatic forces. The other method (Derjaguin *et al.* 1976; Prodi, Santachiara & Prodi 1979) involves the observation of particles moving along a narrow channel, either horizontal or vertical, under the action of a parallel or transverse temperature gradient. A potential difficulty in both of these methods is that the gas through which the particles move may be subject to free convection and thermal creep effects, and corrections for such gas motions may have to be made.

The measurements of thermophoretic velocities by Derjaguin *et al.* (1976) using both the horizontal and vertical slit methods and a jet method were found to be correlated by the formula

$$U_T = -2{\cdot}2\nu \frac{(\nabla T)_x}{T_0} \frac{\left(\frac{k_g}{k_p} + C_t \frac{\lambda}{R}\right)}{\left(1 + 2\frac{k_g}{k_p} + 2C_t \frac{\lambda}{R}\right)}, \tag{17}$$

which is the Derjaguin & Yalamov result with the factor 3 revised downward to 2·2 (implying a value of $C_s \approx 1{\cdot}1$, close to the theoretical value). Although this is the formula most frequently cited in the current literature, because of the questionable nature of the theory underlying this result, plus the adjustment of the constant, it can hardly be regarded as more than an empirical formula. We shall discuss these and other experiments subsequently.

5. Present experiment

Our experimental work on thermophoresis had its inception as part of a study on catalysed combustion in laminar boundary-layer flow over a heated flat plate. As part of this study, it was decided to use LDV to measure the velocity distribution within the boundary layer. It was quickly discovered, however, that this was impracticable because the thermophoretic forces on the seeding particles introduced for the LDV measurements were sufficiently large to cause significant migration of the particles away from the plate, with the result that a substantial portion of the boundary layer was in effect devoid of particles. However, it appeared that, despite the failure of the LDV technique to yield velocity measurements within the inner portions of the boundary layer, the data obtained might prove useful in terms of a quantitative measurement of the thermophoretic force (Goren 1977), and this has in fact turned out to be the case.

The 'particle-free' region which we observed and reported earlier (Schefer *et al.* 1978) is exemplified by the data on particle count rate within the boundary layer shown in figure 1. In the absence of thermophoresis, the particle count rate in a variable-density boundary layer should have the same variation with y as $\rho u/(\rho u)_\infty$, where ρ and u are the fluid density and x component of velocity and the subscript ∞ denotes free-stream conditions. Under the influence of appreciable thermophoretic

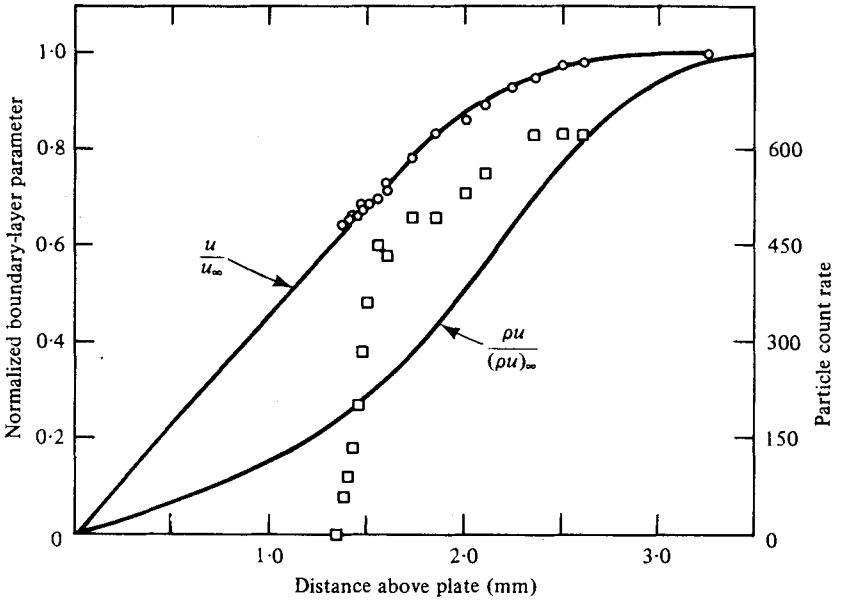

FIGURE 1. Comparison of measured velocity, particle count rate, and mass flux profiles in boundary layer. T_w = 1200 K, U_∞ = 2·62 m s^{-1}. ○, measured velocity; □, particle count rate.

forces, the seed particles through the boundary layer are driven away from the wall. However, owing to the variation in the temperature gradient $\partial T/\partial y$ across the boundary layer, particles close to the wall experience larger thermophoretic forces than those in outer region, and as a consequence the observed particle count rate in the outer region is higher than would be predicted by $\rho u/(\rho u)_\infty$ scaling, but drops to essentially zero approximately midway through the boundary layer. One observes that in the outer region of the boundary layer, where the particle count rate was adequate, the LDV measurements were in good agreement with the theoretically calculated velocity profile. The thickness of the particle-free region, which we define as the locus of the surface within the boundary layer where the particle count rate drops essentially to zero, is proportional to the average thermophoretic force acting on the particles, and thus this average force can be studied under varying conditions of wall temperature T_w and free-stream velocity U_∞ by means of the LDV system.

The details of the experimental set-up have been reported earlier (Robben *et al.* 1977). The flat plate was a 15 mm thick, 75 × 75 mm square quartz plate with a sharp leading edge. Surface heating was achieved through the use of five vacuum-deposited platinum heating strips. The plate was placed in a vertical stream of air originating from a 50 mm diameter convergent nozzle attached to a stagnation chamber. The system was capable of producing values of T_w up to 1300 K, and U_∞ up to about 4 m s^{-1}.

The laser velocimeter was of the intersecting dual-beam type with real fringes. It consisted of an argon ion laser operated at 514 nm, an equal optical path beam splitter which produced a beam separation of 50 mm, and a 250 mm focal-length focusing lens. The radius of the measuring volume created by the intersecting beams was approximately 100 μm. The light scattered from the particles was detected by an RCA 931A photomultiplier oriented at 30° from the forward direction. Doppler bursts were

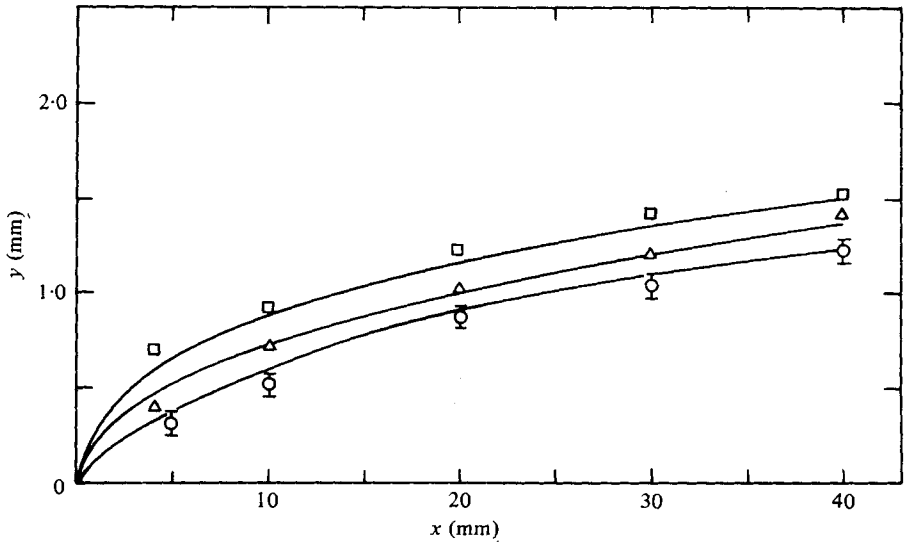

FIGURE 2. Measured thickness of the particle-free region, δ_{PF}, as a function of distance x from the leading edge of the flat plate, with heating commenced at $x = 0$. ○, $T_w = 870$ K, $U_\infty = 3{\cdot}5$ m s^{-1}; △, $T_w = 1170$ K, $U_\infty = 4{\cdot}4$ m s^{-1}; □, $T_w = 1170$ K, $U_\infty = 3{\cdot}0$ m s^{-1}. The curves represent the loci of $u/U_\infty = 0{\cdot}5$ within the three boundary layers.

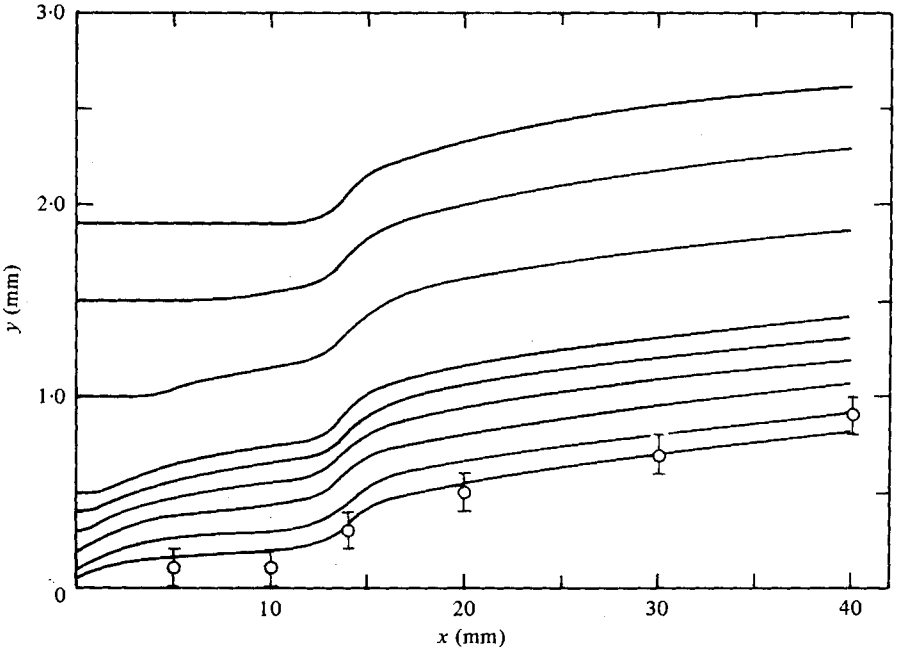

FIGURE 3. Measured δ_{PF} for plate surface heating beginning at $x = 13$ mm; $T_w = 298$ K for $x < 13$ mm, $T_w = 870$ K for $x > 13$ mm, $U_\infty = 3{\cdot}5$ m s^{-1}. Curves are trajectories calculated for test particles inserted into the flow at different y locations upstream of the plate leading edge, using the Brock expression for F_T with $C_s = 1{\cdot}17$.

observed on an oscilloscope, and their frequencies measured with a TSI 1090 tracker unit.

Aluminium oxide particles of nominally 2·0 μm diameter were used as the seed particles. These particles are manufactured (Linde Co.) as abrasives for polishing, and have a quite uniform size distribution. The particles were suspended in water which was atomized by a collision-type atomizer, producing individual particle-carrying droplets which were introduced into the stagnation chamber by an airstream. The water surrounding the particles evaporated rapidly, leaving the particles dispersed throughout the flow exiting from the stagnation chamber. To ensure that the particles did not form into clusters in this process, the size distribution of the particles emerging from the stagnation chamber was measured by means of a 'Virtual Impactor' particle-sizing device developed at the Lawrence Berkeley Laboratory. It was found that 80 % by weight of the particles were less than 3 μm in diameter, the average being approximately 2 μm.

Experimental results were obtained over a range of wall temperatures from 670 to 1280 K, at free-stream velocities of from 1·2 to 4·4 m s^{-1}. The temperature gradient at the wall, $(\nabla T)_{yw}$, was of the order of 10^6 K m^{-1} under these conditions. The Knudsen number λ/R based on a particle radius of 1 μm varied from about 0·15 near the wall to 0·07 in the free stream. Most of the measurements were made with the plate surface heating beginning at the leading edge, but some measurements were obtained with the heating started at 13 mm downstream from the leading edge in order to investigate whether the leading edge had any specific effect on the thickness of the particle-free region.

The outer edge of the particle-free region was established by scanning velocity profiles at different axial stations along the plate, from 4 mm to 40 mm from its leading edge. The LDV system was first set to track in the free stream, where the particle count rate was typically about 600 s^{-1}, and then the probe volume was traversed across the boundary layer towards the plate surface. The boundary of the particle-free region was established as the y location within the boundary layer where the frequency tracker ceased to track a Doppler frequency. The uncertainty in the determination of this location was about 100 μm, which was essentially the diameter of the probe measuring volume.

Typical results for the case of heating over the entire plate surface are shown in figure 2. The particle-free region thickness δ_{PF} appears to scale with that of the hydrodynamic boundary layer, since the loci of $u/U_\infty = 0{\cdot}5$ for the three cases shown fit the data quite nicely. The ratio δ_{PF}/δ_{BL} of the thickness of the particle-free region to the boundary-layer thickness appears to be sensibly independent of T_w and U_∞ at least over the range of values of these parameters encompassed by the data. The error bounds for the data for $T_w = 870$ K are representative of all of the data.

Results for surface heating beginning at $x = 13$ mm are shown in figure 3. (The curves represent a theoretical result which will be described subsequently.) The effect of the leading edge on δ_{PF} may be assessed by comparing the value of δ_{PF} at equal distances downstream from the location where heating was initiated. For example, the value of δ_{PF} at $x = 27$ mm for the data of figure 2 with $U_\infty = 3{\cdot}5$ m s^{-1}, $T_w = 870$ K, may be estimated to be $\delta_{PF} \approx 0{\cdot}96$ mm, whereas from figure 3 we estimate that at $x = 40$ mm, $\delta_{PF} \approx 0{\cdot}90$ mm. These two values of δ_{PF} agree within the uncertainty

of measurement, and thus it may be concluded that the plate leading edge does not have a specific influence on the thickness of the particle-free region.

Comparison with theory

The theoretical calculation of δ_{PF} as a function of x is relatively straightforward, given the magnitudes of the forces F_V and F_T acting on a particle, since $\delta_{PF}(x)$ is analogous to the trajectory of a typical particle entering the boundary layer at a position $y \approx 0$, very close to the wall. The lateral motion of a particle, assuming it to be spherical, is governed by the equation (see Walker *et al.* 1979 and Fernandez & Rosner 1980 for discussions of the Lagrangian formulation of particle motion, particularly justification for the neglect of Brownian diffusion)

$$\tfrac{4}{3}\pi R^3 \rho_p \frac{dv_p}{dt} = F_T + F_V, \tag{18}$$

where ρ_p is the particle density, and v_p the particle velocity relative to the fluid in the y direction. We assume that the particle velocity in the x direction is the same as u, the fluid velocity, so that the x component of the particle relative velocity is zero. If v_p is determined, then, given u and v from boundary-layer calculations, the particle trajectory may be calculated. Since our Knudsen numbers were of the order of 10^{-1}, the viscous forces F_V as given by either the Basset, Stokes–Cunningham or Millikan formulae were about the same. We chose to use the Basset expression. Various expressions available for F_T, as discussed earlier, were employed.

A finite-difference computer code (Schefer 1980) previously developed to solve the equations of fluid flow over a heated plate was modified to calculate particle trajectories. In the finite-difference scheme, the flow field was divided into a rectangular grid of Δx and Δy, of variable grid size. At each $x = m\Delta x$ location, the boundary-layer profile was calculated to obtain the local values of ρ, T, $\partial T/\partial y$, μ, k_g, u and v. Using these local values, the finite-difference form of (18) was solved to obtain v_p. Test particles were inserted in the free stream ahead of the plate evenly spaced at 0·05 mm in y from $y_p = 0{\cdot}05$ mm to 2 mm, thus giving forty separate particle trajectories. Since the laser probe measuring volume was approximately 100 μm in diameter the initial location $y_p = 0{\cdot}05$ mm chosen for the 'wall test particle' represents the minimum y distance for the LDV measurements. For each particle, the y location as a function of x was calculated from $y_{p,n} = y_{p,n-1} + v_p \Delta t$, where $\Delta t = u_{m,n-1}/\Delta x$ and $u_{m,n-1}$ is the flow velocity in the x direction at x-grid location m and particle location $y_{p,n-1}$. Interpolation between mesh points was used to obtain local properties. The particle properties were taken to be $k_p = 30{\cdot}25$ J m^{-1} s^{-1} K^{-1}, and $\rho_p = 4{\cdot}0 \times 10^3$ kg m^{-3}. For these particles, $k_g/k_p = O(10^{-3})$; thus they are representative of the higher conductivity case. The overall uncertainty in the trajectory calculations is estimated to be less than 5 %.

Figure 4 shows a few of the particle trajectories calculated for the case of $T_w = 870$ K, $U_\infty = 3{\cdot}5$ m s^{-1}, with heating beginning at the leading edge. The Brock expression for F_T given by (15) was used (of course, replacing $(\nabla T)_x$ by $\partial T/\partial y$ and using local values of the flow properties obtained from the boundary-layer calculations) with coefficients $C_s = 1{\cdot}17$, $C_m = 1{\cdot}14$ and $C_t = 2{\cdot}18$. The trajectory for the test particle inserted closest to the wall, at $y = 0{\cdot}05$ mm, may be compared with our measured values of δ_{PF}. It can

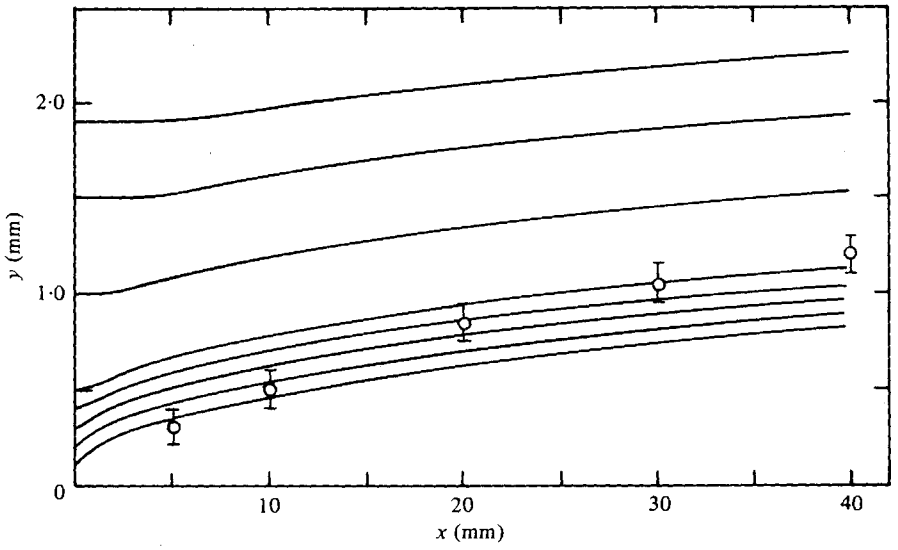

FIGURE 4. Measured δ_{PF} for plate surface heating beginning at $x = 0$. $T_w = 870$ K, $U_\infty = 3{\cdot}5$ m s^{-1}. Curves are trajectories calculated for test particles inserted into the flow at different y locations upstream from the leading edge, using the Brock expression for F_T with $C_s = 1{\cdot}17$.

be seen that, near the leading edge, this wall-particle trajectory is in reasonably good agreement with the data. However, at downstream locations δ_{PF} seems to be larger than is predicted by the calculation. This downstream underprediction of δ_{PF} was also found in other comparisons.

One explanation for the poorer agreement between the calculated wall-particle trajectory and the measured values of δ_{PF} at downstream locations is that the method used for determination of δ_{PF} tends to record the position within the boundary layer where the particle count rate starts to decrease, rather than where the count rate falls to zero. Near the leading edge, the decrease in particle count rate occurs quite abruptly and steeply and therefore the error involved is relatively small. Farther downstream the decrease in particle count rate within the boundary layer occurs more gradually with decreasing distance from the plate surface, and the error in the location of δ_{PF} can be significantly greater. Thus the data in this region can be expected to represent an upper bound on δ_{PF}.

A few of the computed particle trajectories in the case where heating was initiated 13 mm downstream from the leading edge of the plate are shown in figure 3, the expression used for F_T being the same as before. The agreement between the wall-particle trajectory and the measured values of δ_{PF} is very satisfactory, although slight underprediction of δ_{PF} is evident at $x = 40$ mm. It is interesting to note that within the region where there is no wall heating there is still an outward displacement of the particle due to the fluid drag on the particles associated with the v component of velocity.

Wall-particle trajectories for the experimental conditions of figure 3 were also calculated according to the formulae proposed by Derjaguin & Yalamov (1966) (13) and by Derjaguin *et al.* (1976) (17), using the Basset drag formula to convert U_T to F_T.

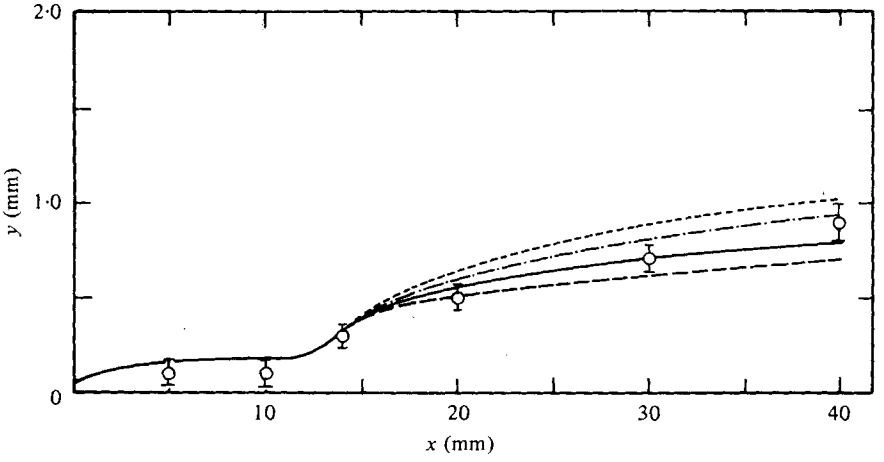

FIGURE 5. Comparison between measured values of δ_{PF} for the experimental conditions of figure 3, and wall particle trajectories calculated according to several formulae for F_T'. Theoretical curves: ——, Brock, $C_s = 1{\cdot}17$; – – –, Brock, $C_s = \frac{3}{4}$; – · – · –, Derjaguin *et al.* (1976), from equation (17); · · · ·, Derjaguin & Yalamov (1966) from equation (13).

These trajectories are plotted in figure 5, together with the trajectories obtained from the Brock formula with $C_s = 1{\cdot}17$ and $\frac{3}{4}$, and the experimental data. The comparison between theory and experiment favours the Brock formula with $C_s = 1{\cdot}17$, although there is not too much difference between the several theoretical curves. The reason for this is that the present experiments are restricted to the Knudsen number range $\lambda/R \lesssim 10^{-1}$, and in this region the theories differ from one another mainly in the value of C_s employed.

6. Dependence of F_T and U_T on λ/R

We have seen that the present experiments do not provide much information on the dependence of F_T or U_T on Knudsen number. We therefore shall examine the results of other experiments in an attempt to assess the usefulness of (15) or (16) in describing the thermophoretic phenomenon over a wide range of λ/R.

Rosenblatt & LaMer were apparently the first investigators to study the thermal forces on individual droplets using a modified Millikan cell. They worked with tricresyl phosphate (TCP), a low-conductivity liquid, in air, and covered the range $0 \leqslant \lambda/R \leqslant 1{\cdot}5$. They concluded that their data were in reasonable agreement with the Epstein formula. A similar conclusion was reached by Saxton & Ranz (1952) using paraffin and castor oil droplets. More recently, measurements were reported by Schmitt on silicone oil droplets in argon ($k_g/k_p = 0{\cdot}135$) which covered the range $0 \leqslant \lambda/R \leqslant 3$. Schmitt's data for the thermophoretic force on six different-sized droplets collapse into one curve (cf. his figures 6 and 7) when expressed in terms of the reduced force $F_T/R^2\nabla T$ *vs.* λ/R. We have plotted his data as the dashed curve in figure 6.

Schadt & Cadle performed experiments similar to Schmitt's on several aerosols,

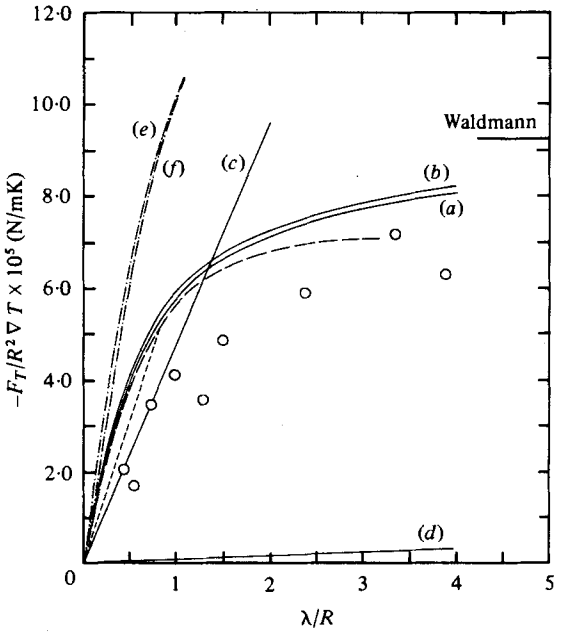

FIGURE 6. Reduced thermophoretic force as a function of Knudsen number. Data: ○, Schadt & Cadle, Hg; - - - -, Schadt & Cadle, TCP; – – – –, Schmitt, silicone oil. Analytical results: ——, equation (15), (*a*) Schadt & Cadle data, (*b*) Schmitt data; ——, Epstein formula, equation (1), (*c*) Schmitt data, (*d*) Schadt & Cadle data; – · – · –, Derjaguin *et al.* (1976), from equation (17), (*e*) oil droplets, (*f*) NaCl.

of both high and low thermal conductivity. Their data on mercury droplets in air ($k_g/k_p = 0{\cdot}00226$) cover the widest range of Knudsen number among the high conductivity aerosols they studied and we have shown their individual data points in figure 6. Schadt & Cadle used the Stokes–Cunningham drag formula to determine the droplet radii, and we have adjusted their data using the Millikan formula instead. Also plotted as a dotted line in the figure is the mean of the data they obtained with TCP droplets. Data on NaCl particles obtained by Jacobson & Brock (1965) in the range $0 \leqslant \lambda/R \leqslant 0{\cdot}6$, which we have not shown, fall about on Schadt & Cadle's TCP data.

For comparison, we have plotted in figure 6 $F_T/R^2\nabla T$ as given by (15) and by Epstein's formula (1) for both the Schmitt and the Schadt & Cadle data. It is seen that whereas the Epstein formula is in rough agreement with the Schmitt data and with Schadt & Cadle's TCP data, at least for $\lambda/R < 1$, it gives values nearly two orders of magnitude smaller than the Schadt & Cadle mercury data. On the other hand, (15) agrees very well with the Schmitt data, and gives values about 20 per cent above the experimental values of Schadt & Cadle, taking into account the Millikan correction to their results. (For the Schmitt data we evaluated $\mu = 4k_g/15\mathscr{R}$, using the experimental value of k_g cited by the author, although it seems to be a little low. If the value of μ calculated from the Lennard–Jones potential were used, the fitting formula curve would be displaced upward about 4 per cent.) The Waldmann $\lambda/R \to \infty$ asymptotes differ slightly for the two plots of (15) because of the differing properties of the gases in which the particles were suspended in the two experiments. We show the Waldmann asymptote corresponding to the Schmitt data.

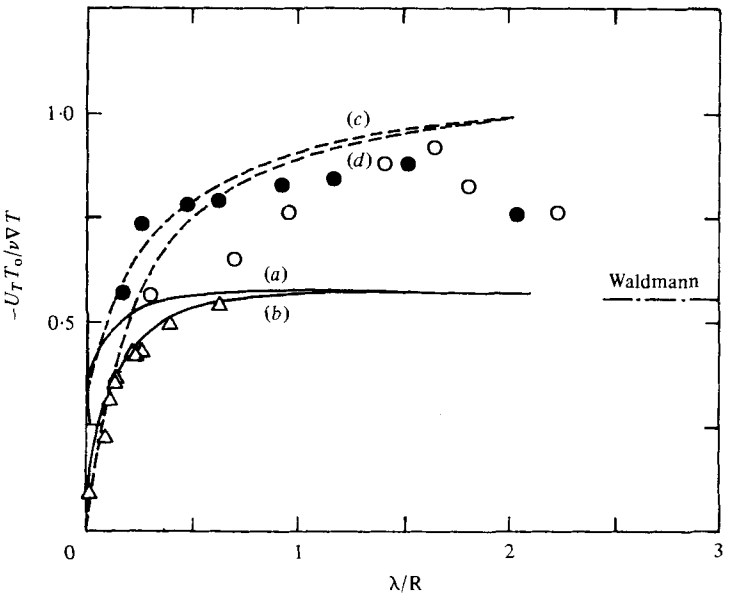

FIGURE 7. Thermophoretic velocity as a function of Knudsen number. Analytical results: ——, equation (16), (*a*) oil droplets, (*b*) NaCl; – – – – equation (17), (*c*) oil droplets; (*d*) NaCl. ○, Derjaguin *et al.* (1976), NaCl; ●, Derjaguin *et al.* (1976), oil droplets; △, Prodi *et al.* (1979), NaCl.

Comparison can also be made with the data of Derjaguin *et al.* (1966, 1976) on oil and NaCl aerosols. These authors report their results in terms of the thermophoretic velocity U_T as shown in figure 7, which is a replot of figure 2 of their paper. Also plotted for comparison are curves giving $U_T T_0/\nu\nabla T$ according to (16) and (17). It is seen that these data are in better agreement with the Derjaguin *et al.* correlation than with the presently proposed fitting formula. The fact that their U_T data fall for the most part considerably above the collisionless limit implies that the corresponding thermal forces exceed $F_{T\infty}$. In fact, if we insert the expression for U_T given by (17) into the Millikan drag formula, we obtain the curves shown in figure 6 identified as Derjaguin *et al.* (1976). However, as an additional comparison, we have also plotted in figure 7 the thermophoretic velocity data of Prodi *et al.* (1979) obtained with NaCl particles. It is seen that these data agree exceedingly well with our fitting formula (16).

Evidently, the data of Derjaguin *et al.* are in substantial disagreement with the Schmitt and Schadt & Cadle data. The correlation formula (17) would appear to have incorrect behaviour for large λ/R since it predicts velocities (and forces) nearly double the collisionless limit values. It is not clear from the information given in their paper how Derjaguin *et al.* (1966) determined the size and speed of fall of their aerosol droplets. The Basset formula, the use of which is implied in the paper by Derjaguin & Yalamov (1965), becomes inaccurate for $\lambda/R \gtrsim 0{\cdot}1$, and this in fact, as noted earlier, fixes the range of validity of the self-consistent hydrodynamic theory. Since, as we have already observed, results such as (17) which derive from arguments based on irreversible thermodynamics cannot in principle yield information beyond that obtained from Navier–Stokes theory, the range of validity of (17) might also be expected to be $0 \leqslant \lambda/R \lesssim 0{\cdot}1$. From a comparison of their correlation formula with Brock's result (12), with $C_s = 1{\cdot}1$ used in both cases, Derjaguin *et al.* (1976)

conclude that the inclusion of isothermal velocity slip (which gives rise to the factor $(1+2C_m\lambda/R)$ in the denominator of (12)) 'drastically impairs the agreement between theory and experiment', by which we understand that they believe that the phenomenon of velocity slip should be ignored. This is an unwarranted conclusion, however, since it is based on the use of Brock's result *with the Basset drag* far beyond its range of applicability.

We are unable to offer an explanation for the discrepancies between the Derjaguin *et al.* data and those of Schmitt, Schadt & Cadle and Prodi *et al.* The first authors suggest that the differences may be ascribed to greater errors due to natural convection inherent in the Millikan cell method as compared to their methods but their arguments are hardly persuasive. The fact that their data appear to asymptote for large λ/R to values considerably in excess of the collisionless limit suggests that the converse might in fact be the case.

Although our fitting formula (15) appears to be reasonably satisfactory for the entire range $0 \leqslant \lambda/R \leqslant \infty$, it is interesting to examine what changes result from assuming that the molecule–surface interactions do not correspond to the perfectly diffuse, complete thermal accommodation case. Drag measurements on the various aerosols used in the thermophoresis studies support the assumption of perfectly diffuse reflexion, which corresponds to $C_m = 1{\cdot}14$. It is, however, conceivable that molecules arriving from regions of the gas having differing temperatures might not fully accommodate to the particle temperature, thus resulting in a value of the thermal accommodation coefficient α less than unity. (See the appendix for the kinetic theory definition of this coefficient.)

In the near-continuum regime, α enters into the values of both C_t and C_s. The first of these is given by Loyalka, for Maxwell molecules, as

$$C_t = \frac{15}{8}\left(\frac{2-\alpha}{\alpha}\right)(1+0{\cdot}1621\alpha) \tag{19}$$

and the second, according to Ivchenko & Yalamov, is given by

$$C_s = \frac{3}{2}\left(\frac{0{\cdot}6264+0{\cdot}3736\alpha}{1{\cdot}2528+0{\cdot}0306\alpha}\right). \tag{20}$$

A reduction in the value of α to less than unity in the near-continuum regime ($\lambda/R \ll 1$) would mainly affect the value of F_T given by (15) through a reduction in the value of C_s, thus lowering the value of F_T. However, for values of λ/R of $O(1)$, since C_t increases as α is decreased, the decrease in C_s would be offset to greater or lesser degree, depending on the value of k_g/k_p, by the increase in the ratio of the two factors containing C_t in the expression for F_T.

On the other hand, it is shown in the appendix to this paper that, if a more general model than was employed by Waldmann is used to analyse the free-molecular thermophoretic drag, a lowering of α results in an increase in F_T in the limit $\lambda/R \to \infty$. Thus it appears that no significant overall improvement in the fit provided by (15) would be achieved by abandoning the very plausible assumption that $\alpha = 1$.

The authors acknowledge with gratitude the contributions of Dr Y. C. Agrawal and Dr F. Robben to this work in its early stages. This work was supported by the Division of Basic Energy Sciences of the U.S. Department of Energy under Contract no. W-7405-ENG-48.

Appendix. Free molecular thermophoretic sphere drag with incomplete thermal accommodation

In order to calculate the free molecular thermophoretic drag force it is necessary to model the manner in which molecules are emitted from the surface. Waldmann chose to use Maxwell's classical model in which a fraction of the molecules are reflected specularly, and the rest are reflected with a Maxwellian distribution characterized by the wall temperature. Waldmann's rather surprising conclusion was that the thermophoretic drag was independent of the fraction specularly reflected. In the subsequent analysis a somewhat different model is chosen. The reflected molecules are assumed to be re-emitted with a Maxwellian distribution specified by a (varying) temperature T_e which will only be equal to the wall temperature if there is complete thermal accommodation. This model assumes complete tangential momentum accommodation but allows for the possibility of incomplete thermal accommodation. This model might be more realistic than Waldmann's for actual particle surfaces with molecules having very different masses from those of the gas molecules, if the particle temperature is sufficiently high. A thermal accommodation coefficient of unity is to be expected for temperatures $\lesssim 500$ K, where significant thicknesses of physisorbed layers of gases are present on surfaces and promote high thermal accommodation, but at higher temperatures, when such layers are desorbed, incomplete accommodation is a possibility.

The sphere is considered at rest in a stream where the distribution function for molecules striking the body is given by the Chapman–Enskog expression (for monatomic molecules)

$$f_{\text{in}} = f_\infty = f_0(1 + D(c^2 - \tfrac{5}{2})\, c_x), \quad c_n < 0, \tag{A 1}$$

where c is the non-dimensional molecular speed and c_n is the velocity normal to the surface measured positive out of the surface and

$$c = \xi/(2kT_0/m)^{\frac{1}{2}}, \tag{A 2}$$

where ξ is the molecular speed and D is the (small) non-dimensional parameter

$$D = \frac{-8k_g}{5\rho_0(2kT_0/m)^{\frac{1}{2}}} \left(\frac{\partial T}{\partial x}\right)_\infty. \tag{A 3}$$

It is assumed that the free-stream temperature gradient is in the x direction. When expressed in terms of the mean free path it is found that

$$D = -(6/\pi^{\frac{1}{2}})\, \lambda(\partial T/\partial x)_\infty / T_0. \tag{A 4}$$

The unperturbed velocity distribution function is given by

$$f_0 = n_0 \left(\frac{m}{2\pi k T_0}\right)^{\frac{3}{2}} \exp(-c^2). \tag{A 5}$$

It is assumed that the molecules are reflected from the surface with a Maxwellian distribution specified by a variable local number density n and temperature T_e, i.e.

$$f_{\text{out}} = n \left(\frac{m}{2\pi k T_e}\right)^{\frac{3}{2}} \exp(-m\xi^2/2kT_e).$$

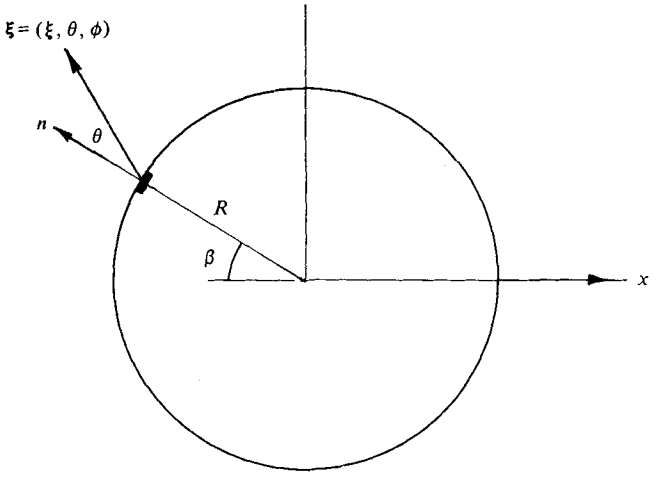

FIGURE 8. Notation for free-molecular integration.

Neglecting second-order small quantities this is written

$$f_{\text{out}} = f_0\left(1+\frac{\Delta n}{n_0}+\frac{\Delta T_e}{T_0}(c^2-\tfrac{3}{2})\right), \quad c_n > 0, \tag{A 6}$$

where

$$\frac{\Delta n}{n_0} = \left(\frac{n-n_0}{n_0}\right) \quad \text{and} \quad \frac{\Delta T_e}{T_0} = \frac{T_e - T_0}{T_0}.$$

In general both $\Delta n/n_0$ and $\Delta T_e/T_0$ are functions of the position on the body which is defined by the angle β, figure 8.

A relationship between $\Delta n/n_0$ and $\Delta T_e/T_e$ is established by imposing the condition that the normal velocity of the gas is zero on the surface of the sphere. This becomes

$$\iiint_{\xi_n<0} f_{\text{in}}\,\xi_n\,d^3\xi + \iiint_{\xi_n>0} f_{\text{out}}\,\xi_n\,d^3\xi \equiv 0 \tag{A 7}$$

and, as there is no net flux due to $f = f_0$,

$$\iiint_{\xi_n<0} f_0\,\xi_n\,Dc_x\,(c^2-\tfrac{5}{2})\,d^3\xi + \iiint_{\xi_n>0} f_0\,\xi_n\left(\frac{\Delta n}{n_0}+\frac{\Delta T}{T_0}(c^2-\tfrac{3}{2})\right)d^3\xi \equiv 0. \tag{A 8}$$

Using the co-ordinate system shown in figure 8

$$\xi_n = (2RT_0)^{\frac{1}{2}}\,c\cos\theta,$$

$$c_x = -c(\cos\theta\cos\beta + \sin\theta\cos\phi\sin\beta) \tag{A 9}$$

and

$$f_0\,d^3\xi = \frac{n_0}{\pi^{\frac{3}{2}}}\exp(-c^2)\,c^2\,dc\sin\theta\,d\theta\,d\phi.$$

The first integral in (A 8) is now readily shown to be zero as

$$\int_0^{2\pi} d\phi\, c_x = -2\pi c \cos\theta \cos\beta$$

and

$$\int_0^{\infty} c^4(c^2 - \tfrac{5}{2})\, e^{-c^2} dc \equiv 0.$$

The second integral in (A 8) is therefore also zero and using

$$\int_0^{\infty} c^5 e^{-c^2} dc = 2\int_0^{\infty} c^3 e^{-c^2} dc$$

it is found that

$$\frac{\Delta n}{n_0} + \frac{\Delta T_e}{T_0}(2 - \tfrac{3}{2}) = 0 \tag{A 10}$$

or

$$\frac{\Delta n}{n_0} = -\frac{1}{2}\left(\frac{\Delta T_e}{T_0}\right).$$

Consequently the outgoing distribution function can be rearranged as

$$f_{\text{out}} = f_0\left(1 + \frac{\Delta T_e}{T_0}(c^2 - 2)\right), \quad c_n > 0. \tag{A 11}$$

The remaining unknown quantity, $\Delta T_e/T_0$, is determined by using the definition of the thermal accommodation coefficient

$$\alpha = \frac{\iiint f(\frac{1}{2}m\xi^2)\, \xi_n\, d^3\xi}{\iiint f_*(\frac{1}{2}m\xi^2)\, \xi_n\, d^3\xi}, \tag{A 12}$$

where f_* has the same value as f for incoming molecules but corresponds to re-emission with a Maxwellian distribution function characterized by the actual surface temperature $T_p(R, \beta)$. In addition T_p has to satisfy

$$\nabla^2 T_p = 0, \quad 0 \leqslant r \leqslant R, \tag{A 13}$$

and the energy balance at the surface,

$$-k_p\left(\frac{\partial T_p}{\partial r}\right)_{r=R} = \iiint f(\tfrac{1}{2}m\xi^2)\, \xi_n\, d^3\xi. \tag{A 14}$$

Using (A 1), (A 9) and (A 11) the energy transport out of the surface reduces to

$$\begin{aligned}\iiint f(\tfrac{1}{2}m\xi^2)\, \xi_n\, d^3\xi &= \rho_0(2kT_0/m)^{\frac{1}{2}}(-5D\cos\beta/16 + (\Delta T_e/T_0)/(2\pi^{\frac{1}{2}})) \\ &= \alpha\rho_0(2kT_0/m)^{\frac{1}{2}}(-5D\cos\beta/16 + (\Delta T_p(R,\beta)/T_0)/(2\pi^{\frac{1}{2}})).\end{aligned} \tag{A 15}$$

The formal solution of (A 13), (A 14) and (A 15) is

$$\frac{\Delta T_p}{T_0} = \frac{T_p - T_0}{T_0} = \left(\frac{r}{R}\right)(\cos\beta)\, H, \tag{A 16}$$

where H is given by

$$H = (5\pi^{\frac{1}{2}}/8)\, D/(1 + 2\pi^{\frac{1}{2}} k_p T_0/(\rho_0 (2kT_0/m)^{\frac{1}{2}} R\alpha)). \tag{A 17}$$

In the free molecular limit the second term in the denominator is $\gg 1$ and

$$H = \left(\frac{5}{16}\right)\left(\frac{D\rho_0 (2kT_0/m)^{\frac{1}{2}} R\alpha}{k_p T_0}\right) = -\frac{1}{2}\frac{k_g R\alpha}{k_p T_0}\left(\frac{\partial T}{\partial x}\right)_\infty \tag{A 18}$$

and (A 16) simplifies to

$$\frac{\Delta T_p}{T_0} = \frac{1}{2}\frac{k_g}{k_p}\frac{\alpha}{T_0}\left(\frac{\partial T}{\partial x}\right)_\infty$$

using $x = -r\cos\beta$. However, it is sufficient to note that, as $\lambda/R \to \infty$, $H/D \to 0$ so (A 15) reduces to

$$\frac{\Delta T_e}{T_0} = \frac{5\pi^{\frac{1}{2}}}{8}(1-\alpha)\cos\beta. \tag{A 19}$$

Finally the force per unit area in the x direction on an element of the surface is given by

$$\frac{dF_x}{dA} = \iiint f(-m\xi_x)\,\xi_n\, d^3\xi, \tag{A 20}$$

which on using (A 1), (A 8) and (A 20) reduces to

$$\frac{dF_x}{dA} = (\rho_0 kT_0/m)\left(\frac{D}{4\pi^{\frac{1}{2}}}(1+\cos^2\beta) + \frac{5\pi^{\frac{1}{2}}}{32} D\cos^2\beta(1-\alpha)\right). \tag{A 21}$$

The total force in the x direction is then

$$\begin{aligned} F_x &= \int_0^\pi \left(\frac{dF_x}{dA}\right)(2\pi R^2 \sin\beta)\, d\beta \\ &= (2\pi R^2)(\rho_0 kT_0/m)\left(\frac{D}{4\pi^{\frac{1}{2}}}(2+\tfrac{2}{3}) + \frac{5\pi^{\frac{1}{2}}}{32} D(\tfrac{2}{3})(1-\alpha)\right). \end{aligned}$$

Using the definition of D and $\bar{c} = (8kT_0/m)^{\frac{1}{2}}$ this reduces to

$$F_x = -\left(\frac{32}{15}\right)\left(\frac{R^2}{\bar{c}}\right) k_g \left(\frac{\partial T}{\partial x}\right)\left(1 + \frac{5\pi}{32}(1-\alpha)\right). \tag{A 22}$$

The term $(5\pi/32)(1-\alpha)$ represents an increase in the free molecular drag over the value obtained by Waldmann in the case when (effectively) $\alpha = 1$ or $T_e = T_p(R,\beta) = T_0$.

REFERENCES

Annis, B. K. 1972 *J. Chem. Phys.* **57**, 2898.

Basset, A. B. 1888 *A Treatise on Hydrodynamics*, vol. 2, p. 270. Cambridge: Deighton, Bell & Co. (Reprinted by Dover, 1961.)

Brock, J. R. 1962 *J. Colloid Sci.* **17**, 768.

Derjaguin, B. V., Rabinovich, Ya. I., Storozhilova, A. I. & Scherbina, G. I. 1976 *J. Colloid Interface Sci.* **57**, 451.

Derjaguin, B. V., Storozhilova, A. I. & Rabinovich, Ya. I. 1966 *J. Colloid Interface Sci.* **21**, 35.

DERJAGUIN, B. V. & YALAMOV, YU. 1965 *J. Colloid Sci.* **20**, 555.

DERJAGUIN, B. V. & YALAMOV, YU. 1966 *J. Colloid Sci.* **21**, 256.

DURST, F., MELLING, A. & WHITELAW, J. H. 1976 *Principles and Practice of Laser-Doppler Anemometry*. Academic.

DWYER, H. A. 1967 *Phys. Fluids* **10**, 976.

EPSTEIN, P. S. 1929 *Z. Phys.* **54**, 537.

FERNANDEZ, J. & ROSNER, D. E. 1980 Inertial deposition of particles revisited and extended. Presented at *3rd Int. Levich Conf., Madrid.* (To appear in *Physicochem. Hydro.*)

GORELOV, S. L. 1976 *Isv. Akad. Nauk S.S.S.R., Mekh. Zhidkosti i Gaza* **5**, 182.

GOREN, S. L. 1977 *J. Colloid Interface Sci.* **61**, 77.

IVCHENKO, I. N. & YALAMOV, YU. I. 1971 *Russian J. Phys. Chem.* **45**, 317.

JACOBSON, S. & BROCK, J. R. 1965 *J. Colloid Sci.* **20**, 544.

KENNARD, E. H. 1938 *Kinetic Theory of Gases*. McGraw-Hill.

LOYALKA, S. K. 1968 *J. Chem. Phys.* **48**, 5432.

LOYALKA, S. K. & CIPOLLA, J. W. 1971 *Phys. Fluids* **14**, 1656.

LOYALKA, S. K. & FERZIGER, J. H. 1967 *Phys. Fluids* **10**, 1833.

PRODI, F., SANTACHIARA, G. & PRODI, V. 1979 *J. Aerosol Sci.* **10**, 421.

ROBBEN, F., SCHEFER, R., AGRAWAL, Y. & NAMER, I. 1977 Catalyzed combustion in a flat plate boundary layer. I. Experimental measurements and comparison with numerical calculations. *Western States Section, Combustion Inst. Paper* no. 77–37, Stanford, CA. (Also *Lawrence Berkeley Lab. Rep.* 6841.)

ROSENBLATT, P. & LAMER, V. K. 1946 *Phys. Rev.* **70**, 385.

SAXTON, R. L. & RANZ, W. E. 1952 *J. Appl. Phys.* **23**, 917.

SCHADT, C. F. & CADLE, R. D. 1961 *J. Phys. Chem.* **65**, 1689.

SCHEFER, R. W. 1980 *Combustion and Flame* (in the press).

SCHEFER, R. W., AGRAWAL, Y., CHENG, R. K., ROBBEN, F. & TALBOT, L. 1978 Motion of particles in a thermal boundary layer. *Lawrence Berkeley Lab. Rep.* 7843.

SCHMITT, K. H. 1959 *Z. Naturf.* A **14**, 870.

SONE, Y. & AOKI, K. 1977 In *Rarefied Gas Dynamics* (ed. J. L. Potter), Progress in Astronautics and Aeronautics, vol. 51, part 1, pp. 417–433. A.I.A.A.

SPRINGER, G. S. 1970 *J. Colloid Interface Sci.* **34**, 215.

VESTNER, H., KÜBEL, M. & WALDMANN, L. 1975 *Nuovo Cim.* B **25**, 405.

WALDMANN, L. 1959 *Z. Naturf.* A **14**, 590.

WALDMANN, L. 1961 In *Rarefied Gas Dynamics* (ed. L. Talbot), p. 323. Academic.

WALKER, K. L., HOMSY, G. M. & GEYLING, F. T. 1979 *J. Colloid Interface Sci.* **69**, 138.